OUKA

**The University of Osaka
Institutional Knowledge Archive**

Title	Spectroscopic Characterization of Smart Spraying Plasmas for Thermal Barrier Coatings Preparation
Author(s)	Kobayashi, Akira; Ishibashi, Norifumi
Citation	Transactions of JWRI. 2005, 34(1), p. 25-30
Version Type	VoR
URL	https://doi.org/10.18910/8415
rights	
Note	

Spectroscopic Characterization of Smart Spraying Plasmas for Thermal Barrier Coatings Preparation

ZHANG Jialiang* and KOBAYASHI Akira**

Abstract

Thermal Barrier Coatings (TBCs) are frequently prepared by the thermal plasma spraying method. The performance of the TBC coating is strongly determined by process parameters, such as particle temperature and velocity, plasma temperature and range. In this paper, an optical emission spectroscopy system is used to determine the excitation temperature generated by a gas tunnel type cascade arc plasma gun and a high speed CCD camera is used to image the spatial profile of plasma emission intensity in the form of successive frames at a time resolution of 30μs and to get the plasma range. As both of them are believed to be the key factors for determining the molten surface status and velocity of the sprayed particles, the plasma temperature and range are presented as the tendencies dependent on discharge power and gas flow rate. Based on these tendencies, the radiation power and heat flux from the plasma are evaluated, the plasma velocity at the exit of the generation gun has been solved theoretically. In order to show the effect of powder injection on the plasma plume, when Al_2O_3 powder is injected by the argon carrier, the plasma temperature is calculated from the emission spectra of aluminum atoms melted away from the powder particles and is lower than that obtained from argon spectra.

KEY WORDS: (Spraying plasma plume), (Spatial emission profile), (Thermal barrier coatings), (Excitation temperature), (Energy dissipation pattern).

1. Introduction

The controlling technology research for arc discharge plasma is currently at an early stage and few ideas on arc plasma processing control have been presented. Thinking about the reasons, one attributes the complicated instability of arc discharge to be the biggest barrier while the lack of diagnostic tools suitable for arc plasma is another [1].On the other hand, arc discharge plasma is attracting more and more attention from researchers and industrial manufacturers, because arc plasmas allow attainment of much higher output than low pressure glow discharge plasmas [2]. More complete understanding of arc discharge and related processes are necessary to improve the performance of the arc plasma manufacturing processes, in particular, thermal plasma spraying.

Thermal spraying technology based on thermal plasma torch has been used to produce ceramic, metal and plastic coatings for various applications such as wear resistance, high temperature insulation and corrosion protection, and is becoming the most promising application of arc plasmas because of high temperature and enthalpy [3]. Although TBCs have been prepared by many methods such as Chemical Vapor Deposition (CVD) from gas phase precursors and reactive magnetron sputtering, thermal plasma spraying still appears to be the most efficient technique for TBC preparation because of its high production efficiency and low cost. However, it has been reported that the performance of thermal sprayed coatings is strongly determined by the plasma process parameters, such as particle velocity, plasma temperature and length [4], which are

too many to control and optimize for high reproducibility of the sprayed coating performance. Nevertheless, all of the plasma process parameters are believed to influence the input discharge power and consequently power dissipation to different kinds of energy, which can be evaluated from the thermal spraying plasma geometry and the plasma flowing velocity. Therefore, diagnostics on plasma torch geometry and its flowing velocity field should be the key and basic factor for designing the operation mode of the thermal plasma spraying process. There have been a lot of researches on arc plasma and thermal plasma spraying in various publications [5, 6], but few systematic researches on the thermal spraying processes exist, especially on the relation between the thermal plasma parameters and overall discharge conditions.

One of the authors has developed a gas tunnel type plasma spraying technique to prepare TBCs [7][8]. The resultant YSZ coatings take on a graded porosity microstructure, which has the benefit of low spallation rate of the bond layers and sintering rate of porosities [9][10]. The prepared Al_2O_3 hard coatings appear very hard, with Vickers Hardness higher than 1200. However, the diagnostic research situation on the novel kind of spraying plasma is almost the same as that of other kinds of thermal plasmas, showing the same diagnostic difficulty, and therefore a systematic investigation on its operation features is needed. Generally speaking, in all kinds of thermal plasmas, kinetic processes are dominated by electron collisions and the so-called local thermal equilibrium (LTE) hypothesis holds true especially when the electron density is high enough. Therefore, optical emission spectroscopy should be a suitable tool to show

the temperature and spatial profile of thermal plasmas.

In this paper, an optical spectroscopy system was used to investigate the excitation temperature of the first-stage plasma and the two-stage cascade plasma plume as functions of plasma discharge conditions. At the same time, in order to related the discharge power to the plasma temperature, the plasma torch geometry was also be studied via a high speed CCD camera. From the CCD movie frames, the kinetic velocity of the sprayed particle, if injected, can be obtained by the trace length of the particles passing through the plasma plume. The movie frames recorded by the camera are also used to relate the discharge condition and the plasma energy dissipation processes.

2. Experimental Description

The diagnostic experiments were conducted on a novel spraying system equipped with an electrical meter assembly and an optical diagnostic system. The novel plasma spraying system consists of a two-stage arc discharge configuration and forms a cascade arc plasma torch structure, in which the generated plasma column should be denser than any conventional mono-stage arc plasma. Diagnostics were carried out respectively on the first-stage discharge and then on the two-stage cascade discharge, because the first-stage discharge is important for the ignition and stability of the second-stage discharge, while the second stage is the power amplification of the first-stage discharge.

2.1 Atmospheric Plasma Spraying Assembly (APS)

The gas tunnel type plasma spraying system has a specially designed third anode, which is characterized by some gas channels on its wall in such a pattern that the gas flows injects into the hollow cavity of the anode and forms a gas tunnel in the axis region. The plasma firstly forming in the hollow anode and then emitting like a flame outside the exit would be well confined in the tunnel due to thermal pinch effect and be much higher in temperature and more stable than traditional free-standing arc torches [11].

Figure 1 shows a schematic drawing of the plasma spraying setup, which consists of one trigger cathode rod, one hollow cathode and one hollow anode. More detail of the system is presented in [12]. Facing the torch, a two-dimension movable substrate holder is equipped to vary the distance between substrates and the torch exit. The first-stage of the system is powered by a DC power source which can provide current as high as 100A and power as high as 10KW and triggered by a
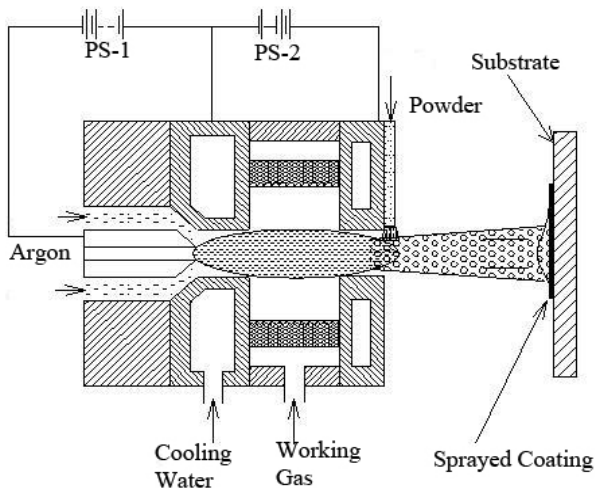
Fig.1 Schematic of the Plasma Spraying Setup.

high voltage as high as 3KV at pulsation frequency of 120Hz, while the second-stage is powered by another more powerful DC supply that can output current as high as 500A and power of 30KW to enhance the plasma. For the two stages of discharge, two gas inlets are used to feed working gas or carrier gas. The working gas for the first stage is fed through the rear inlet around the trigger electrode, while the carrier gas for the second stage is fed from the channels on the vortex anode wall. For spraying, some kind of precursor powder is injected into plasma columns near the plasma exit by carrier gas at certain controllable feeding rates.

Although the spraying system is always operated in the atmosphere, it is installed in a shielding chamber to avoid the powder residues from polluting the Lab and to shield the torch from the ambience air. Some view ports are open on the chamber wall and are sealed with glass windows for optical and spectroscopic diagnostics of the plasma spraying processes.

In the present research, working argon gas is fed into the gap between the first-stage electrode pair at a nominal gas flow rate of 50l/min and also carrier gas of argon is fed into the vortex anode cavity at a nominal rate of 150l/min. Normally, based on the present configuration, the first-stage arc is successfully run with arc voltage of 40-55V and current of 60-80A, while the second-stage discharge is also successfully maintained with voltage of 30-40V and current of 300-450A.

2.2 Configuration of Optical Emission Spectrometer

There are two diagnostic systems for discharge and plasma parameters of the gas tunnel type plasma attached to the setup, one of which is an optical emission spectroscopy system for plasma spectral emission profile and excitation temperature, the other is a discharge voltage and current meter assembly attached to the power sources. From the electrical meter assembly, the total discharge power and plasma power density can be calculated. The spectroscopy system consists of three parts: the optical collection system, a transmission fiber bundle and a grating spectrometer consisting of a monochromator and a detector with a photo multiplication tube (PMT). The optical fiber bundle is used to sample the optical emission through the view window, which is put at the focal region of the imaging lens group, conjugate with the plasma plumes.

The resolution of the spectrometer is nominally 0.05nm and its spectral response ranges from 350nm to 800nm. The PMT spectral response in range of 400nm to 500nm is almost uniform so that spectral intensity correction is not needed for argon spectra in the range of 410-430nm. A self-made potential meter is used to indicate the sampling position of the fiber bundle. A high-speed CCD camera is used to show the movie of the plasma radiance intensity at a time resolution of 30μs, from which the geometry of the plasma plumes can be constructed.

3. Results and Discussions

The present investigation firstly aims at the plasma column generated by the first-stage discharge and then at the plasma jets by the two-stage discharge, focusing on the temperature and emission profile of the plasma plumes and then analysis of the energy dissipation pattern. Because the main component of the working gas is argon, most attention is concentrated on the argon atom spectra. The optical collection position of the diagnostic system is always focused on the central region of columns outside the plasma exit.

3.1 Investigation of the First-Stage Discharge
3.1.1 Typical optical emission spectra from argon plasma

Figure 2 is a sample spectrum from the plasma generated in pure argon with flow rate of 50L/min by the first-stage
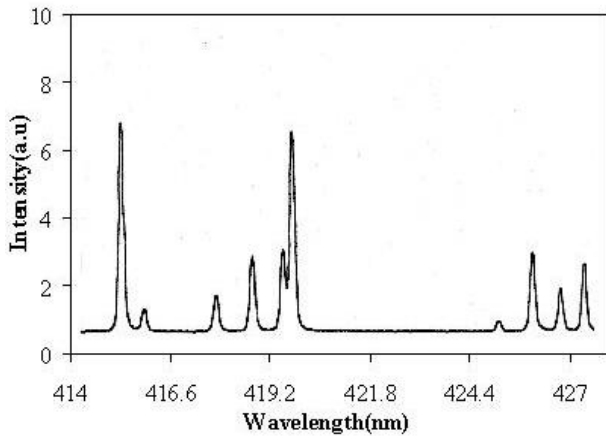
Fig.2 A spectra of argon plasma at current of 60A

Fig.4 Discharge V-I characteristic vs. gas flow rate.

discharge with current of 60A, and shows only argon atom spectral lines. In the plasma column region, no electric field exists and thus no energetic electrons and argon ions are generated [13]. Consequently, the emissive species in the plasma column is excited from the metastable argon atoms by the residual energetic electrons or inherited directly from the discharge region. Normally speaking, there should be an abundance of excited argon ions in the discharge region. However, excited argon ions usually have very short lifetime and are difficult to retain in the plasma column region, which is why there is no argon ion spectral line in the sample spectrum. The argon atom lines lie mainly in wavelength ranges of 400nm to 450nm and 690nm to 810nm. Because the response limit of the PMT, only the lines in the shorter wavelength range are recorded. In the spectrum, 11 argon spectral lines appear and only 7 of the 11 lines are chosen to calculate the excitation temperature, because multiple atom lines whose wavelength are too close can not be resolved from one other or by neighbor argon atom line. The transition constants of the argon lines are given in Ref [14] for excitation temperatures obtainment [15].

3.1.2 Voltage-current relation of the first-stage plasma

The discharge power is found to increase when the discharge current increases, meanwhile increasing almost proportionally when gas flow rate rises, as shown in **Figure 3**, but the plasma temperature does not greatly vary with the gas flow rate. **Figure 4** illustrates that the discharge voltage drops with increasing discharge current when the gas flow is kept constant, and on the
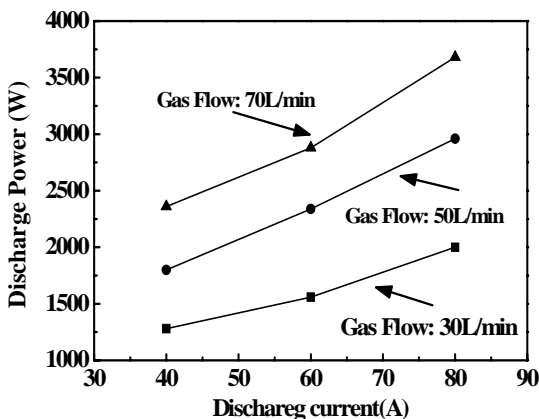
other hand, the discharge voltage increases almost linearly with the gas flow rate when discharge current is kept constant. When discharge current increases, the electron number density in discharge column increases and therefore the collision rate between electrons and gas atoms becomes higher, which leads to a higher efficiency for thermal ionization of the discharge and easier maintenance of the discharge. That is why the discharge voltage decreases with higher discharge current. However, if the gas flow rate becomes higher, the mean free-path of electrons in the discharge region becomes shorter and hence the discharge voltage has to increase to maintain the ionization rate in the discharge.

3.1.3 Correspondence of the excitation temperature on discharge conditions

Figure 5 shows the excitation temperature of the first-stage plasma with discharge current as the variable. In thermal plasmas, any kinetic processes are dominated by electron collisions and the so-called local thermal equilibrium (LTE) hypothesis holds true especially when the electron density is high enough. Based on the belief that the argon atom population in its excited state is under Boltzmann equilibrium with the electron gas, the spectra of argon atom are suitable for obtaining the excitation temperature via the Boltzmann Plot Scheme. The temperature is measured from the axial region of the plasma columns 2 cm away from the plasma exit. From the curves, the excitation temperature is slightly lifted when the discharge power increases, which means that a critical temperature for arc discharge exists and it is difficult to make the temperature
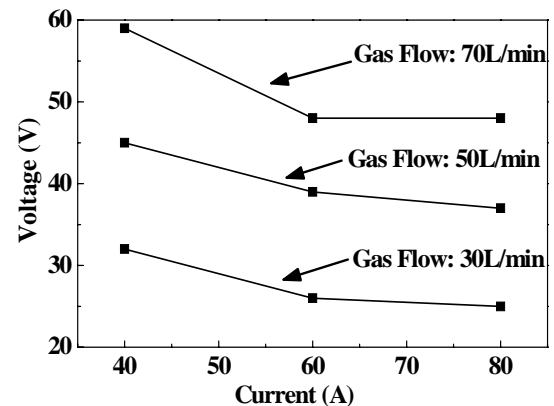

Fig.3 Discharge power vs. discharge current and gas flow rate.

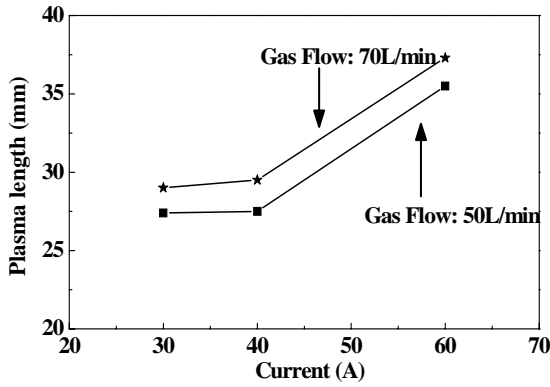**Fig.5** Discharge V-I characteristic vs. gas flow rate.

Fig.6 Plasma length with arc current and gas flow rate.

higher than the critical temperature by increasing power. However it was found that the temperature remained almost the same when the gas flow rate increased. The slight increase of plasma temperature versus discharge current is due to the competition between the discharge power increase and the electron energy decrease occurring simultaneously with a discharge current increase, because the increment of ionization and excitation degree in the plasma and discharge voltage lowering take place simultaneously with the discharge current. The gas flow rate increment leads to the discharge power increment linearly, but it results in increment in collision possibility between electron and argon atoms and therefore in the plasma length extension but the plasma temperature, which is why the plasma temperature remained constant when the gas flow rate increased.

3.1.4 Spatial profile of the first-stage plasma versus discharge conditions

Figure 6 presents the length of pure argon plasma jet versus discharge conditions, and is obtained from the frames of running argon plasma taken by the high speed CCD camera at a time resolution of 30μs. From the frames, the maximum diameter of the profile is about 10mm and is a little wider than the torch gun exit diameter of 8 mm, which is due to the radial diffusion of the plasma column. The slight diameter expansion indicates that the thermal diffusion of the plasma is much slower than the plasma flow. As gas flow rate increases, the plasma length increases uniformly if the discharge current kept constant. But when the gas flow is kept constant, the length increases non-linearly with the discharge current, because higher current input raises the plasma temperature but lowers the discharge voltage and therefore discharge power and power density increase non-linearly with the current increment.

3.1.5 Energy dissipation pattern in the first-stage plasma

The plasma plume energy is originally obtained from the electrical energy input and dissipates in such kinds of paths as radiation, heat loss at the electrode surfaces, heat flux and conversion to kinetic energy and excitation energy of the plume, which can be expressed as the following:

$$P_{in} = P_{rad} + P_{loss} + P_{flux} + P_k + P_{exc}, \qquad (1)$$

Here, P_{in}, the input electrical power; P_{rad}, the radiation power of the plasma; P_{loss}, the power of heat loss at the electrode walls; P_{flux}, the energy flux at the plasma exit; P_k, the kinetic energy flux of the plume and P_{exc}, the excitation power for excited species formation.

The heat loss power, P_{loss} at the electrode wall can be evaluated from the overall energy efficiency for the plasma generation, η, as $P_{loss} = P_{in}(1-\eta)$, while P_{exc}, the line emission

power of the discharge, is included partially in the radiation power P_{rad} and the residual part is temporally neglected only for simplification in the present analysis. Considering that the plasma plumes are high temperature systems, a black-body radiation model is used to evaluate the radiation power according to Stefans Law: $P_{rad} = \sigma T^4 S$ (σ, the Stefan Factor; T, temperature of the plasma; S, the surface area of the plasma column). As for the heat flux power, $P_{flux} = \rho R C_v T$, according to the law of continuity of fluid, where ρ and R refer to the mass density and gas flow rate of the working gas argon, C_v the isometric specific heat of argon and T the plasma temperature. As the result of the above evaluation, plasma kinetic energy flux can be expressed as the following:

$$P_k = 0.5 \, \rho R v^2 = P_{in}\eta - P_{rad} - P_{flux} \qquad (2)$$

The following is an example case to show the above evaluation scheme of energy dissipation in the first-stage discharge. The temperature of the plasma from the first-stage discharge is about 6500K at the central region, when the gas flow rate is 50L/min and the discharge power is 2340W. The corresponding diameter and length of the plasma plume are about 10mm and 36mm respectively, which lead to a cross-section of $1.1cm^2$ at the exit of the cone shape of the plume. After taking the mass density and specific heat of argon in the standard state to be 1.78g/L and 0.31J/gK, the P_{rad} and P_{flux} are calculated to be about 450W and 1150W. In the meanwhile, the overall energy efficiency of the first-stage discharge is normally about 75% and hence the total power contained by the plasma plume is $P_{in}\eta = 1700W$. So, the plasma kinetic power of about 100W(=1700W-450W-1150W) accelerates the plasma plume to a directional velocity of 370m/s, while the injection velocity of working gas is about 17m/s because of the gas flow rate of 50L/min and the discharge channel diameter of 8mm. In conclusion, the plasma flowing velocity is mostly originated from the discharge energy.

3.2 Investigation of the Cascade Arc Gas Tunnel Type Spraying Plasma

3.2.1 Some characteristics of the plasma jet

Figure 7 shows a picture of the argon plasma plume formed by the two-stage cascade discharge enhanced by the vortex anode when the discharge current is 450A and the argon flow rate is 150L/min, and is recorded by the use of a high-speed CCD camera at a time resolution of 30us. This indicates that the diameter and length of the plume are 15mm and 55mm. **Figure 8** shows a spectrum from the plasma jet formed by the two-stage cascade discharge with Al_2O_3 powder injection at a feeding rate of 2g/min, which shows 8 argon lines and 3 aluminum ion lines also with some small unidentified peaks from the impurities of Al_2O_3 powders. The spectrum indicates that the injected Al_2O_3 powders are melted, or even vaporized and sputtered by the high temperature argon torches and gaseous Al atoms are generated. Although it is believed that there is no electrical field or energetic electrons in the plume
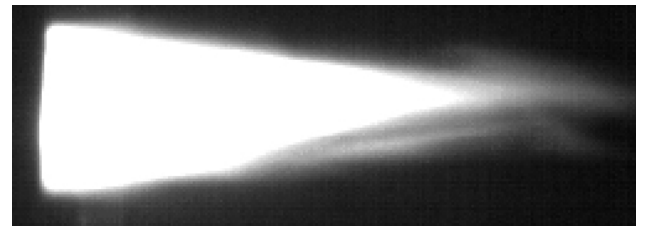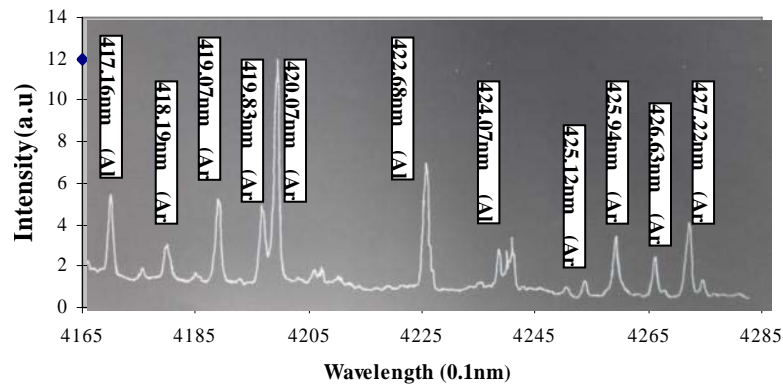

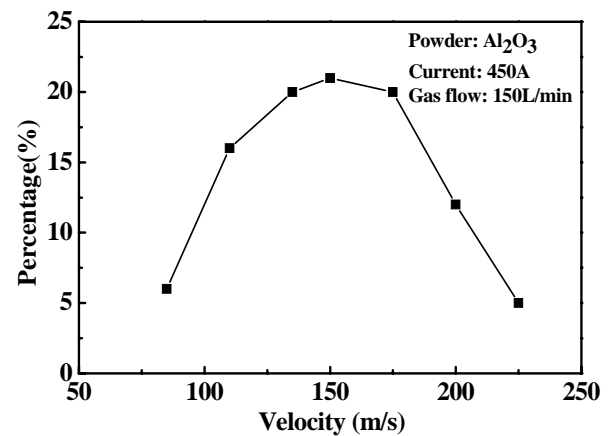**Fig.7** A picture of the plasma with current of 450A.

Fig.8 Spectra of argon plasma jet with Al_2O_3 powder

Fig.9 A picture of plasma plume with Al_2O_3 powder

Fig.10 Powder particle velocity distribution

region, lots of metastable argon atoms are available, which possess an excess energy of 11.5eV enough for the Penning process to excite and ionize the Al atoms. Because of the Penning process, the emission spectra of those metal atom species are markedly enhanced and can be used to obtain the plasma temperature together with the argon spectra. Based on the spectrum in Fig.7, the temperature for the plasma with discharge current of 450A and gas flow rate of 150L/min is estimated to be 8400K and 7300K respectively from the argon lines and Al lines. The different temperature is a hint that the injected powers are not heated by the plasma to be isothermal because the residual time of powders in the plasma plume is not long enough.

3.2.2 Velocity Distribution of the Powder Particles Injected into the Plasma Plumes

Figure 9 is an image recorded by the high-speed CCD camera at a time resolution of 30us to show the powder particle trajectories illuminated by the plasma jet discharged also at current of 450A and gas flow rate of 150L/min. From the image, the powders travel with straight trajectories during the camera exposure interval. The different lengths of the trajectories means that the powder velocity is not uniform, from which the powder velocity distribution can be calculated as shown in **Figure 10** and the average powder velocity is estimated to be 152m/s that is much lower that the plasma jet flow velocity. The particle velocity, much lower than the plume velocity, also shows that the powders are not accelerated efficiently by the plasma flow. As shown in Fig.9, when sprayed powders are injected into the plasma jet, the diameter of the plume keeps

almost the same as that without powder injection, while the plume length shrinks down to about 40mm since the injected powders absorb energy from the plasma jet.

4. Conclusions

Some results on the optical emission spectroscopic diagnostics of novel gas tunnel type argon plasma plume have been obtained as follows:

(1) The temperature tendency with the discharge power as the variable shows that a critical high temperature for sustaining arc plasma is needed and that the real plasma temperature is always close to the critical temperature, although the temperature slightly increases with increasing discharge power.

(2) The emission profile pictures of the plasmas generated only by the first-stage discharge indicate that the thermal diffusion of the plume is much slower than the plume flow, but that the plasma plume length increases non-linearly with increasing discharge current and gas flow rate, because the energy dissipation pattern and branching ratios in the discharge area vary with the discharge power and gas flow rate.

(3) The energy dissipation scheme in the first-stage discharge is theoretically analyzed basing on a simple model. The analysis shows that the most part of the input discharge energy transforms into the enthalpy of the plasma jet. Some part of the energy is converted into radiation and only a small part into the plume kinetic energy to form the directional plume velocity.

(4) When Al_2O_3 powders are injected into the plasma jet

generated by the two-stage discharge, the plasma temperature can be obtained from the spectrum of argon atoms or aluminum atoms, which shows difference between the argon temperature and aluminum temperature. The injected powders are not heated isothermal to the plasma because the powders reside in the plasma for a too short residence time.

(5) Although the residue of powders in the plasma is short, powders are accelerated to a high average speed of about 152m/s by the plasma and travel along straight trajectories in the plasma jet. However, the powder velocity is much lower than that of the plasma velocity because the acceleration by the plasma is not enough.

References

[1] R. Hidaka et al*., Japan. J. Appl. Phys*, Vol 26(10) (1987) pp L1724-L1726

[2] Q.S.Yu and H.K.Yasuda, *Plasma Chemistry and Plasma Processing*, Vol 18 (1998), pp461-479

[3] J. H. Zaat, *Ann. Rev. Material*, Vol 13 (1983) pp9-13

[4] A.Kucuk, C.C.Berndt, U.Senturk, R.S.Lima and C.R.C. Lima, *Mat. Sci. Eng*. Vol A284 (2000) pp29-40

[5] A.Kucuk, C.C.Berndt, U.Senturk and R.S. Lima, *Mat. Sci. Eng*. Vol A284 (2000) pp41-50

[6] Q. S. Yu and H. K.Yasuda, *Plasma Chemistry and Plasma Processing*, Vol 18 (1998), pp461-479

[7] Y.Arata, A.Kobayashi, Y.Habara and S. Jing, *Trans. of JWRI*, Vol.15-2 (1986) pp227-231.

[8] A.Kobayashi, S.Kurihara, Y.Habara and Y.Arata, *J.Weld. Soc. Jpn.,* Vol 8 (1990), pp457-462.

[9] A.Kobayashi, *Surface and Coating Technology,* Vol.90, (1990) pp.197-202.

[10] A. Kobayashi, *Proc. Of ITSC*., (1992), pp57-62.

[11] Y.Arata and A.Kobayashi, *Journal of High Temperature Society*, Vol 11(1) (1985) pp 18-28.

[12] A.Kobayashi, *J.High Temp. Soc.* Vol 11(3) (1985) pp124-131

[13] Y.P.Raizer, *Gas Discharge Physics*, Springer-Verlag, Germany, 1991

[14] J.R. Fuhr and W.L.Wiese, *NIST Atomic Transition Probability Tables, CRC Handbook of Chemistry and Physics* 78 (edited by D.R. Lide), CRC Press, Boca Raton, FL, 1998.

[15] W.C.Martin and W.L.Wiese, *Atomic Spectroscopy, Chapter 10 in Molecular, Atomic and Optical Physics Handbook* (Edited by G.W.F.Drake), AIP press, Woodbury, NY, 1996.